Dispersionless motion and ratchet effect in a square-wave-driven inertial periodic potential system

2009 J. Phys.: Condens. Matter 21 175409

(http://iopscience.iop.org/0953-8984/21/17/175409)

IOP Publishing Journal of Physics: Condensed Matter

J. Phys.: Condens. Matter **21** (2009) 175409 (9pp) doi:10.1088/0953-8984/21/17/175409

Dispersionless motion and ratchet effect in a square-wave-driven inertial periodic potential system

S Saikia[1,2] **and Mangal C Mahato**[1]

[1] Department of Physics, North-Eastern Hill University, Shillong 793022, India
[2] Department of Physics, St Anthony's College, Shillong 793001, India

E-mail: mangal@nehu.ac.in

Received 3 December 2008, in final form 12 March 2009
Published 30 March 2009
Online at stacks.iop.org/JPhysCM/21/175409

Abstract

The underdamped Langevin equation of motion of a particle, in a symmetric periodic potential and subjected to a symmetric periodic forcing with mean zero over a period, with nonuniform friction, is solved numerically. The particle is shown to acquire a steady state mean velocity at asymptotically large timescales. At these large timescales the position dispersion grows proportionally with time, t, allowing for calculating the steady state diffusion coefficient D. Interestingly, D shows a peaking behaviour around the same F_0 where the net current peaks. The net (ratchet) current, however, turns out to be largely coherent. At an intermediate timescale, which bridges the small timescale behaviour of dispersion $\sim t^2$ to the large time one, the system shows periodic oscillation between dispersionless and steeply growing dispersion depending on the amplitude and frequency of the forcing. The contribution of these different dispersion regimes to ratchet current is analysed.

1. Introduction

The investigation of particle motion in periodic potentials has obvious relevance in condensed matter studies. Motion of ions in a crystalline lattice is a case in point. Stochasticity in the motion is naturally introduced at nonzero temperatures. In these environments the particle motion can be approximately described by a Langevin equation with suitable model potentials. Depending on the problem at hand the motion is either considered heavily damped, almost undamped, or in the intermediate situation mildly damped (or underdamped). In many a situation in the former two extreme cases the Langevin equation (or the corresponding Fokker–Planck equation) becomes amenable to analytical solution. However, in the underdamped situation, barring a few special cases, numerical methods are used to solve the equation of motion of the particle [1]. Owing to various kinds of errors and approximations involved in these (numerical) methods, exact quantitative solutions are not possible. However, the method can reveal useful qualitative trends in the behaviour of the particle motion. For instance, recently it was shown [2] that a Brownian particle, moving in an asymmetric but periodic potential and subjected to a symmetric periodic external drive (which adds to zero when averaged over a period), acquires a net motion when the parameters of the problem are chosen suitably. Such a net particle current without the application of any net external bias or potential gradient in the presence of thermal noise is called a thermal ratchet current and the system giving such a current is termed as a thermal ratchet [3]. Here the equilibrium condition of detailed balance is not applicable because the system was driven far away from equilibrium by rocking it periodically in the presence of noise. It was further shown that this system can even exhibit absolute negative mobility [4]. This prediction has already been found to be true experimentally [5]. It shows that in underdamped conditions or in the inertial regime diverse possibilities can be (qualitatively) uncovered by (numerically) solving the appropriate equations of motion.

In the above important examples [2, 4] the potential asymmetry was one of the necessary conditions for the realization of ratchet current. The particle had to surmount the same potential barrier on either direction; only the slopes leading to the top of the barrier differed. A sinusoidal potential, for example, having no such asymmetry would not have yielded the ratchet current. In the present work, we consider similar particle motion in a sinusoidal potential

$V(x) = -V_0 \sin(kx)$. However, instead of a uniform friction coefficient of the medium we consider a model nonuniform space-dependent friction coefficient $\gamma(x)$ of the medium. In particular, we consider a sinusoidally varying $\gamma(x) = \gamma_0(1 - \lambda \sin(kx + \phi))$ exactly similar to the potential but with a phase lag, ϕ. A simple illustrative example of the model can be imagined as a stationary pressure wave established in air giving a periodic $\gamma(x)$ for particle motion along x. An array of ions with the periodicity of $\gamma(x)$ but shifted a little to give a phase lag ϕ will just fit our model for a charged particle motion along x. Here the potential is symmetric and periodic. However, the directional symmetry of the system is broken by a phase shift in the similarly periodic $\gamma(x)$. The model form of a periodically varying friction $\gamma(x)$ has been justified earlier from mode-coupling theory of adatom motion on the surface of a crystal of identical atoms [6]. Also, the equation of motion has a direct correspondence with the resistively and capacitatively shunted junction (RCSJ) model of Josephson junctions; the term describing the nonuniformity of friction having an one-to-one correspondence with the '$\cos\phi$' term in the RCSJ model [7]. Apart from the close analogy with the RCSJ model of Josephson junctions, the inhomogeneous systems with nonuniform diffusion coefficients have been investigated earlier by Landauer [8] and Büttiker [9]. Büttiker has shown that a particle moving in a one-dimensional periodic potential with a similarly periodic diffusion coefficient, but with a phase difference will experience an effective constant force in one direction. Blanter and Büttiker obtained a ratchet effect [10] in a system with similarly varying nonuniform temperature and hence nonuniform diffusion coefficient. The same has been obtained later in a detailed work by Benjamin and Kawai [11] who consider similarly and simultaneously varying periodic temperature and friction in space in the overdamped limit. However, as stated earlier, in this work we consider the friction coefficient to be nonuniform, keeping the temperature uniform. Since the diffusion coefficient is determined by the friction coefficient either separately or together with the temperature, the arguments of Büttiker [9] hold equally in the present case too. There is a difference, however, between the role played by friction inhomogeneity and temperature inhomogeneity. Through the pioneering 'blowtorch' work of Landauer, a temperature inhomogeneity giving a current is a natural consequence [8, 10]. But in the case of friction inhomogeneity, no such obvious inference can be drawn. Temperature along with the potential function determines the static (equilibrium) particle density distribution irrespective of the spatial variation of friction. In other words, frictional inhomogeneity has no effect in determining the static density distribution of particles. Temperature nonuniformity can result in unidirectional net particle current even without the application of external forcings as has been clearly shown in [10], whereas the effect of frictional nonuniformity can be envisaged only in the dynamic situation [12]. The effect of frictional inhomogeneity can manifest itself in two ways. Wherever the friction is large in each period, particle movement gets damped and hence the particles spend more time there. This effectively changes the density distribution. For instance, for $\phi \neq 0, \pi$, the friction coefficient will be different immediately on the left side of the potential peak than on the corresponding immediate right of the peak. Hence, in the periodic (potential) situation it will appear (in the dynamic situation) as though a static force has been applied in order to bring about the change in the distribution [9]. On the other hand, since the particle spends more time in the regions where friction is large, they become more prone to absorb the thermal energy of the immediate environment and hence will effectively have higher probability to surmount the potential barrier for motion [10]. These two competing aspects can give rise to interesting complex behaviour of the particle currents (see, for example, figure 4 of [12]) in periodic potential systems. In the present work, we investigate a number of interesting phenomena exhibited by ratchet current in these inhomogeneous periodic systems. We drive the system with a square-wave periodic field. The reason for choosing a square-wave field as opposed to a sinusoidal field will become clear as we proceed. The resulting Langevin equation is solved numerically. We obtain a particle current and properties associated with it in the parameter space of external field amplitude F_0, the average friction coefficient γ_0, the phase lag ϕ and the temperature T. Since it is a formidable task to explore the entire parameter space, we present results only for some regions of a few sections of this space where an appreciable ratchet current is obtained.

The ratchet current $\bar{v}$ is obtained for ϕ ($\neq n\pi$, with integral n) in the steady state situation which is achieved in the asymptotic time limit. In our case we observe particle motion for a long time t such that the position dispersion $\langle(\Delta x(t))^2\rangle$ averaged over many similar trajectories approach $\sim t$. Thus, we calculate the diffusion constant D using the relation $\langle(\Delta x(t))^2\rangle = 2Dt$ for given γ_0, T, and ϕ. D shows nonmonotonic behaviour with the field amplitude F_0 and it peaks around a value of F_0 where $\bar{v}$ attains a maximum. That is to say, the ratchet current is maximized when the system is most diffusive. To compare the extent of this diffusive spread with the directional average displacement, a quantity Péclet number, $P_e = \frac{\bar{x}^2}{Dt}$, the ratio of the square of mean displacement $\bar{x}$ in time t to half the square of diffusive spread in the same time interval t [14] is calculated. Our calculation shows that in the region where the ratchet current is appreciable, and in particular where $\bar{v}$ peaks, P_e is much larger than 2, indicating that the transport is coherent.

The current in the explored parameter region, however, is not large enough to obtain (practically) useful work; when a small load is applied against current the current either reduces to a small level or starts flowing in the direction of the applied load. Thus, in the given circumstances, no appreciable useful work can be extracted from this inhomogeneous (frictional) ratchet. However, even in the absence of any external load the particle keeps moving against the frictional resistance. Leaving out the symmetric diffusive part of the motion the particle's unidirectional (ratchet) current $\bar{v}$ is maintained against the average frictional force. The *Stokes efficiency*, η_S, which is the ratio of this work (that the ratchet performs against the frictional drag) to the total energy pumped into the system from the source of the external forcings, is also calculated.

An expression for η_S has been derived earlier [2, 14, 15] which involves $\bar{v}$ as well as the second moment of the velocity

v calculated from the probability distribution $P(v)$ of the velocity $v(t)$ recorded all through the trajectory of the particle. We have calculated η_S as a function of the amplitude of the applied forcing. η_S shows a peak, not coinciding with that of the ratchet current. The distribution $P(v)$ is almost symmetric about $v = 0$ and the velocity dispersion grows monotonically, approaching to be linear in F_0 at large F_0.

Recently, it has been reported [16] that in a tilted periodic potential an underdamped particle motion shows a remarkable dispersionless behaviour in the intermediate-time regime for a range of constant tilt values, F_0. In this regime the majority of particles appear to move coherently with a constant speed roughly equal to $\frac{F_0}{\gamma_0}$. In the present work we show that, when the system is driven by a square-wave forcing of appropriate amplitude and frequency, such dispersionless behaviour with added richness can be observed. The dispersionless behaviour corresponding to the constant tilt periodic potential gets punctuated and oscillatory behaviour of dispersion of different kinds, depending on the frequency of the periodic drive, naturally emerges. Interestingly, however, contrary to expectations, the transient coherent particle motion does not contribute positively to the largely coherent steady state ratchet current in this system.

In section 2 the basic equation of motion used in this model calculation will be presented. Section 3 will be devoted to the presentation of the detailed results of our numerical calculation. In section 4 we shall conclude with a discussion.

2. The model

In this work we drive the system periodically by a symmetric square-wave forcing. The choice of square-wave forcing, instead of a sinusoidal forcing, is to make a direct contact with the adiabatically driven case. In the adiabatic drive case the particle motion was studied, keeping the tilt of the periodic potential constant and the net current for two opposing directions of the same magnitude of tilt was calculated. The calculation of the current for a constant tilt was carried out using the matrix continued fraction method (MCFM) as well as using the numerical Langevin dynamics [13].

The matrix continued fraction method was developed by Risken and co-workers [1]. The method involves solving the Fokker–Planck equation governing the time evolution of the probability density function $W(x, v, t)$ of particle position x with velocity $v(=\frac{dx}{dt})$ at time t. The distribution function $W(x, v, t)$ is expanded in series in terms of Hermite functions $\psi_n(v)$ with expansion coefficients $C_n(x, t)$, as $W(x, v, t) = \psi_0 \sum_{n=0}^{\infty} C_n(x, t)\psi_n(v)$. The Fokker–Planck equation is thus transformed into an infinite system of coupled differential equations for the expansion coefficients. The infinite system of equations is truncated and is put in the form of a vector recurrence relation of the expansion coefficients. This recurrence relation is solved by a continued fraction method for matrices in the steady state approximation to obtain the Fourier components of the expansion coefficients C_n, from which the different physical quantities of interest are calculated. The MCFM is extended to suit the present problem in references [12, 13].

The constant tilt case shows dispersionless motion in the intermediate regime as represented earlier [16]. Thus the square-wave drive provides an opportunity to study the dispersionless motion at finite frequencies. In the present case we consider the forcing $F(t)$ as

$$F(t) = \pm F_0, \qquad (2nT_\Omega \leqslant t < (2n+1)T_\Omega),$$
$$= \mp F_0, \qquad ((2n+1)T_\Omega \leqslant t < 2(n+1)T_\Omega),$$

where T_Ω is the half-period of forcing (and which corresponds to a time interval after which the sign of F_0 is changed) and $n = 0, 1, 2, \ldots$. The motion of a particle of mass m moving in a periodic potential $V(x) = -V_0 \sin(kx)$ in a medium with friction coefficient $\gamma(x) = \gamma_0(1 - \lambda \sin(kx + \phi))$ with $0 \leqslant \lambda < 1$ and subjected to a square-wave forcing $F(t)$ is described by the Langevin equation:

$$m\frac{d^2x}{dt^2} = -\gamma(x)\frac{dx}{dt} - \frac{\partial V(x)}{\partial x} + F(t) + \sqrt{\gamma(x)T}\xi(t). \quad (2.1)$$

Here T is the temperature in units of the Boltzmann constant k_B. The Gaussian distributed fluctuating forces $\xi(t)$ satisfy the statistics: $\langle\xi(t)\rangle = 0$ and $\langle\xi(t)\xi(t')\rangle = 2\delta(t - t')$. For convenience, we write down equation (2.1) in dimensionless units by setting $m = 1$, $V_0 = 1$, $k = 1$ so that $T = 2$ corresponds to an energy equivalent equal to the potential barrier height at $F_0 = 0$. The Langevin equation, with reduced variables denoted again now by the same symbols, is written as

$$\frac{d^2x}{dt^2} = -\gamma(x)\frac{dx}{dt} + \cos x + F(t) + \sqrt{\gamma(x)T}\xi(t), \quad (2.2)$$

where $\gamma(x) = \gamma_0(1-\lambda \sin(x+\phi))$. Thus the periodicity of the potential $V(x)$ and also the friction coefficient γ is 2π[3]. The potential barrier between any two consecutive wells of $V(x)$ persists for all $F_0 < 1$ and it just disappears at the critical field value $F_0 = F_c = 1$. The noise variable, in the same symbol ξ, satisfies exactly similar statistics as earlier.

Equation (2.2) is solved numerically (with given initial conditions) to obtain the trajectory $x(t)$ of the particle for various values of the parameters F_0, γ_0 and T. Also, the steady state mean velocity $\bar{v}$ of the particle is obtained as

$$\bar{v} = \left\langle \lim_{t\to\infty} \frac{x(t)}{t} \right\rangle, \quad (2.3)$$

where the average $\langle\cdots\rangle$ is evaluated over many trajectories. The mean velocity is also calculated alternatively from the numerically obtained distribution $P(v)$ of velocities giving almost identical results.

3. Numerical results

The Langevin equation (2.2) is solved numerically using two methods: fourth-order Runge–Kutta [17] and Heun's method (for solving ordinary differential equations). We take a time

[3] The parameter scaling is different from that of Machura *et al*, where [2] the forcing amplitude a is equivalent to π times the amplitude F_0 in our case. The total potential barrier height (at $a = 0$) is ∼1, whereas in this work it is 2. However, the noise strength D_0 in [2] is the same as the temperature T used here.

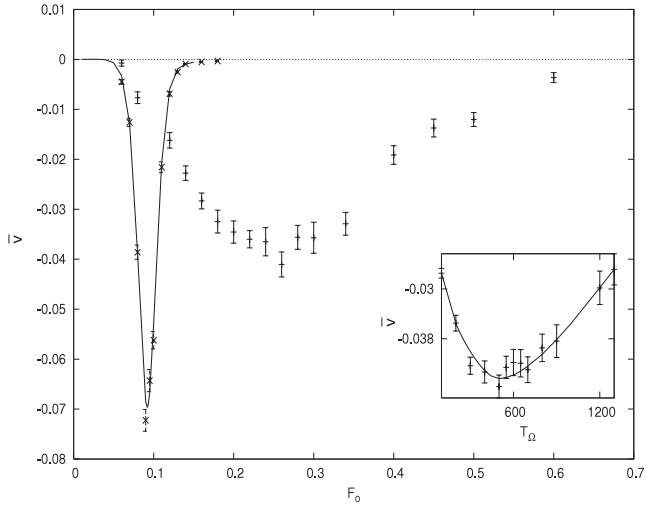

Figure 1. This shows the variation of $\bar{v}$ with F_0 for the adiabatic case. The results obtained by MCFM (continuous line) and simulation (crosses with error bars) are put together for comparison. The MCFM could not be used for F_0 beyond the plotted range. The plus signs with error bars correspond to the square drive case with parameter values $\gamma_o = 0.035$, $\phi = 0.35$ and $T = 0.4$ for $T_\Omega = 1000$. The zero line is given for reference. The inset shows the variation of $\bar{v}$ with T_Ω: simulation data (points with error bars) for $F_0 = 0.26$ and for the same γ_0, T and ϕ values. The fitted curve to the data points is given just to guide the eye.

step interval of 0.001 during which the fluctuating force $\xi(t)$, obtained from a Gaussian distributed random number appropriate to temperature T, is considered as constant and the equation solved as an initial value problem. In the next interval another random number is called on to use as the value of ξ and the process repeated. A careful observation of the individual trajectories of the particle shows that by $t = 10^4$ the particle completely loses its memory of the initial condition it had started with. When we look for steady state solutions the trajectory is generally allowed to run for a maximum time $t = 10^7$. Therefore, for steady state evaluation for $\bar{v}$, etc, the results become independent of initial conditions. The (Runge–Kutta) method had earlier been used and obtained correct results [18] in a similar situation. Also, the Runge–Kutta and Heun's methods were checked against results obtained earlier for the adiabatic case (using the matrix continued fraction method) and found to compare closely (figure 1). Heun's method, when applied in similar situations, takes much less time than the Runge–Kutta method and yields qualitatively as good a result (figure 1). With this confidence in our numerical procedures, we apply either one or the other of these two numerical schemes as the situation demands. We take $\lambda = 0.9$ all through our calculation in the following.

The motion of the particle is governed by the applied square-wave forcing $F(t)$. As $F(t)$ changes periodically so does the position of the particle. In view of this effect we start our simulation at $t = 0$ alternately with $F(0) = +|F_0|$ (first, third, fifth, etc) and $-|F_0|$ (second, fourth, sixth, etc) trajectories. This gives a nice nonoscillating (and initial condition independent) variation of overall average position when finally averaged over a large even number of trajectories. However, while calculating the position dispersions or velocity dispersions at a given time t, the even (beginning with $F = -|F_0|$) and odd (beginning with $F = +|F_0|$) numbered trajectories are treated separately to calculate the deviations from their respective mean values.

3.1. The ratchet current

An appreciable ratchet current $\bar{v}$ is obtained in a small range of F_0 with a peak in an intermediate F_0 for given γ_0, T and ϕ. The variation of $\bar{v}$ as a function of the amplitude F_0 of the applied square-wave forcing $F(t)$, with a frequency ($=\frac{1}{2T_\Omega}$) of 5×10^{-4} cycles per unit time, is shown (figure 1) for $\gamma_0 = 0.035$ and temperature $T = 0.4$. Also, for comparison the algebraic sum, $\Sigma\bar{v}(F_0) = \bar{v}(+|F_0|) + \bar{v}(-|F_0|)$ with applied forces $+|F_0|$ and $-|F_0|$, called the ratchet current in the adiabatic limit, is plotted as a function of F_0. The ratchet current in the adiabatic limit ($T_\Omega \to \infty$) is calculated (by solving the Fokker–Planck equation corresponding to equation (2.2)) using the matrix continued fraction method (continuous line in figure 1) developed by Risken and co-workers [1] and adapted in [12, 13] to suit the present case. The current is also calculated numerically by solving the same Langevin equation (crosses with error bars in figure 1). The adiabatic current calculated by using the two methods agrees quite well. The range of F_0 over which the ratchet current is obtained in the square-wave drive case (using numerical methods) is much wider [$0.05 < F_0 < 0.7$] compared to the adiabatic drive condition [$0.05 < F_0 < 0.15$] and the peak current occurs at a larger F_0 value. The range, though wider, still remains well below F_c, the critical field at which the potential barrier to motion just disappears. The current is, therefore, essentially aided by thermal noise.

The ratchet current $\bar{v}$ also shows nonmonotonic behaviour as a function of the period of the drive. In the inset (figure 1) we plot the variation of $\bar{v}$ as a function of the time period of the drive for $F_0 = 0.26$, $\gamma_0 = 0.035$ and $T = 0.4$. For these parameter values the current $\bar{v}$ peaks at a value of $T_\Omega \approx 500$. For the comparison of timescales, it may be noted that for an equivalent RCSJ model of Josephson junctions (with typical junction capacitance $C = 0.5 \times 10^{-12}$ F and critical current $I_c = 10^{-9}$ C s^{-1}) the characteristic Josephson plasma frequency ω_J turns out to be about 10^3 times larger than the drive frequency ($\frac{1}{2T_\Omega}$) corresponding to $T_\Omega = 1000$. In this sense we obtain an appreciable ratchet current only for very slow drives. It should, however, be noted that in the infinitely slow adiabatic case the ratchet current is effectively zero for $F_0 > 0.15$ for $\gamma_0 = 0.035$ at $T = 0.4$ and $\phi = 0.35$.

3.2. The steady state dispersions

The position dispersions $\langle(\Delta x(t))^2\rangle$, where $\Delta x(t) = x(t) - \langle x(t)\rangle$, are evaluated over a large number of trajectories for various values of F_0, and $T_\Omega = 1000$. It is found that the dispersions fit nicely to

$$\log[\langle(\Delta x(t))^2\rangle] = \log(t) + \log(2D), \qquad (3.1)$$

for large t, typically $t > 10^5$.

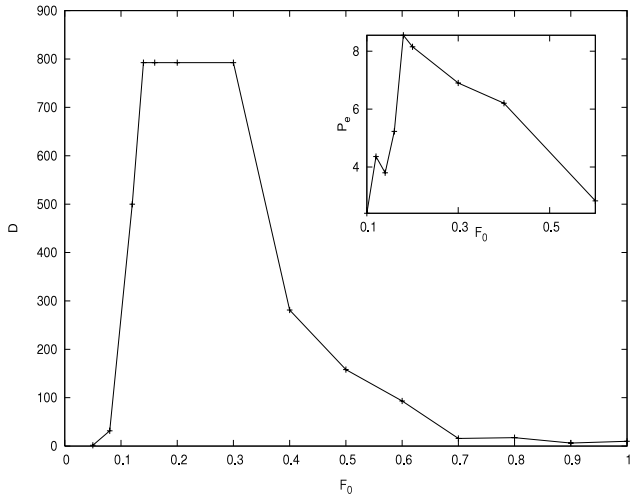

Figure 2. The variation of the diffusion constant D as a function of the driving amplitude F_0 for $\gamma_0 = 0.035$, $T = 0.4$ and $\phi = 0.35$ with $T_\Omega = 1000$. The inset shows the variation of the corresponding Péclet number P_e with F_0.

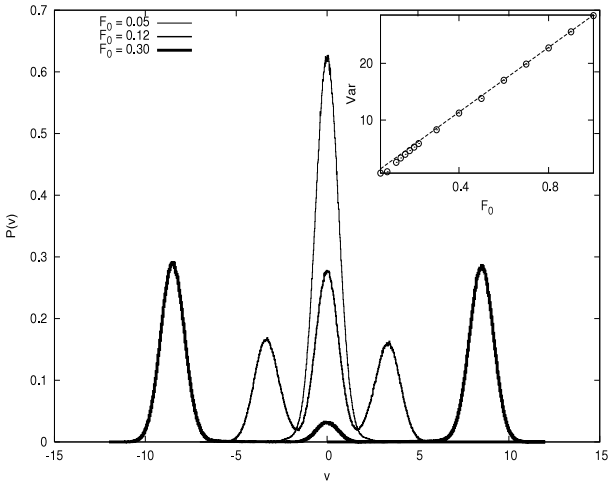

Figure 3. Plot of velocity distribution $P(v)$ for three values of driving amplitudes $F_0 = 0.05$, 0.12 and 0.30 and $\phi = 0.35$. The figure in the inset shows the variance of velocities as a function of F_0 fitted with a straight line to show the linear growth of variance at large F_0.

From the linear fit of the graphs we calculate the diffusion constants $D(F_0)$ and the result is shown in figure 2. The diffusion constant has a large value between $F \approx 0.15$ and 0.35. The peak height is quite large ≈800. As F_0 is increased D decreases sharply and becomes smaller than 50 (which is less than 10% of its peak value) for $F_0 > 0.7$. This $[0.15 \leqslant F_0 \leqslant 0.35]$ is also the region where the ratchet current $\bar{v}$ is appreciable. The Péclet number, P_e, as defined earlier, is also calculated as a function of F_0. They are plotted in the inset of figure 2. It is clear from the figure that in the same region $P_e (=2(\frac{\bar{x}(t)^2}{\langle \Delta x(t)^2 \rangle}))$ is also much larger than 2. This indicates that in the region $[0.15 \leqslant F_0 \leqslant 0.35]$ the particle motion is highly diffusive but concomitantly it is greatly coherent too. This is also indicated equivalently by the observation that, even though the position dispersions (fluctuations) are large, the relative fluctuations of position in this region are considerably lower $(\frac{\sqrt{\langle \Delta x(t)^2 \rangle}}{\bar{x}(t)} < 1)$. As indicated by the result in the adiabatic case (figure 3 [12]) this range of F_0 of coherent motion is expected to shift as the value of γ_0 is changed.

Although our system is different from that of Machura *et al* [2], at this point it would be interesting to make a comparison with their result. They observe that for their low temperature case $D_0 = 0.01$ in the vicinity of $a \approx 0.6$ the velocity fluctuation underwent a rapid change (figure 1a of [2]). To translate this to our case (see footnote 3) $a \approx 0.6$ is equivalent to $F_0 \approx 0.2$ and, given their potential barrier being just about half of the value in our case, one should expect the peaking of velocity dispersion to occur below $F_0 = 0.4$. Taking into consideration our temperature being 40 times 0.01 the phenomena should occur much below $F_0 = 0.4$. In this sense the region $[0.15 \leqslant F_0 \leqslant 0.35]$ seems quite reasonable. Also, $\bar{v}$ of figure 3a of [2] at $D_0 = 0.4$ make a good comparison with figure 1 in our case. However, as mentioned earlier the two systems are quite different in basics to have an exact comparison.

The velocity distribution $P(v)$ also shows interesting behaviour. In figure 3 we plot $P(v)$ for three values of F_0. A sharp peak which is almost indistinguishable from a Gaussian centred at $v = 0$ for small $F_0 = 0.05$, gets split up into three peaks for $F_0 = 0.12$, and similarly for $F_0 = 0.30$, with the central peak gradually diminishing. This shows a behaviour, including the nearly linear growth of the variance with F_0 (inset figure 3), quite similar to what has been reported earlier in a different system [2]. There is, however, one difference. The side peaks of $P(v)$ in our calculation have their origin in the running states of the particle. It is, perhaps, due to the low frequency square-wave drive, instead of the sinusoidal drive, that for as low an amplitude as $F_0 = 0.3$ we get three disjoint velocity bands and at $F_0 = 0.6$ we get just two bands, the central band being almost unpopulated. The three peaks, for example for $F_0 = 0.3$, could be fitted to a combination of three Gaussians. With a cursory look, the left and right Gaussians barely show much difference. However

$$\langle v \rangle = \int_{-\infty}^{\infty} v P(v)\, \mathrm{d}v \tag{3.2}$$

gives approximately the same value as $\bar{v}$ and $\langle v \rangle (F_0)$ showing exactly the same nature as $\bar{v}(F_0)$ (figure 4). It is to be noted that the maximum ratchet current occurs (figure 1) for F_0 at which $P(v)$ shows a transition from a three-peak form to a two-peak one. In this transitional range the frictional asymmetry shows the maximum contrast in responding to the field. In the case where the intrawell motion dominates the ratchet current is low and again when there is only running states (at large F_0) the frictional asymmetry becomes ineffective. These observations are corroborated by the velocity distributions in the adiabatic case, where again maximum difference in current occurs at the transitional period from a two-peak distribution to a single-peak (running state only) distribution. For the adiabatic case the transitional range occurs at lower F_0 values. In the square-wave drive case, the transitional region is shifted to higher F_0,

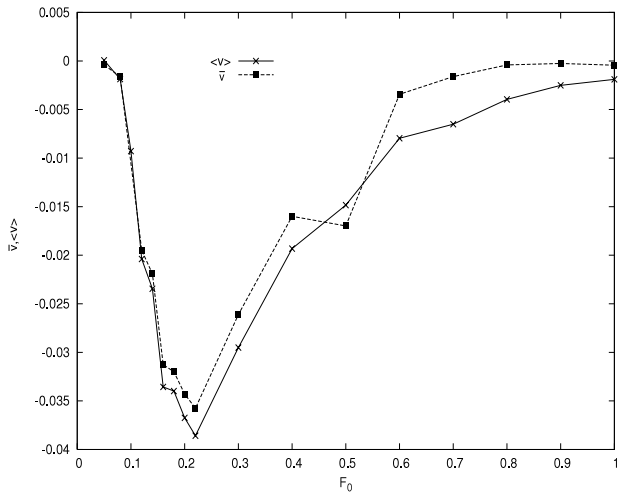

Figure 4. This shows the variation of the steady state mean velocity $\bar{v}$, equation (2.3), and $\langle v\rangle$, equation (3.2), for the same parameter values as in figure 2.

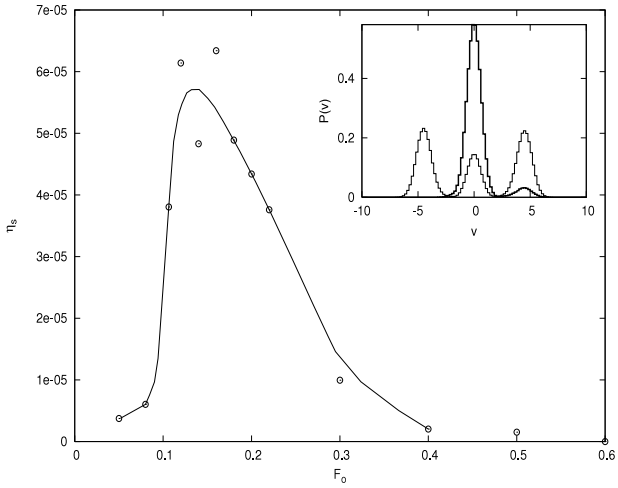

Figure 5. This shows Stokes efficiency, η_S as a function of F_0 for the same parameter values as in figure 2. Simulation data points (circles) fitted with a curve to guide the eye. The inset shows the difference in the velocity distribution for symmetric (three peaks) and asymmetric drive for the same value of $F_0 = 0.16$ and $\tau = 2000$ with $\alpha = 0.2$.

because, when the direction of F_0 is changed, the particles reverse their direction of motion too, and hence have enough chance to get locked into a potential well. This shift in F_0 is responsible for shifting the peak of the current maximum for the square drive case as shown in figure 1.

3.3. The efficiency of ratchet performance

From the velocity distribution $P(v)$ we calculate the Stokes efficiency, η_S, defined as [2]

$$\eta_S = \frac{\langle v\rangle^2}{|\langle v^2\rangle - T|}, \tag{3.3}$$

as a function of F_0. Figure 5 shows that η_S is larger in the same range of F_0 where it shows larger $\bar{v}$. The peak of η_S, however, does not occur at the same position as the peak of $\bar{v}$. It is, however, to be noted that the plotted figure is calculated from averages over a small number ($\sim$20) of ensembles because it is computationally quite expensive to obtain results for the steady state (maximum $t = 10^7$) and hence not feasible to obtain averaging over a larger number of ensembles. Though the qualitative behaviour is encouraging the efficiencies are small $\sim 10^{-5}$. In the adiabatic drive case (figure 8, [13]) we have found that Stokes efficiency depends on various parameter values: γ_0, T, etc. The efficiency shown here is for a small $\gamma_0 = 0.035$, $T_\Omega = 1000$ and $T = 0.4$ where the current is also very low. The efficiency of this symmetrically driven system can, however, be improved to a good extent by an optimal choice of these parameters.

An inertial ratchet driven by a zero mean asymmetric drive can, however, give a highly efficient performance compared to the symmetrically driven ratchet. For example, when the system is driven by a field

$$\begin{aligned} F(t) &= \pm F_0, \qquad (2nT_\Omega \leqslant t < (n+\alpha)2T_\Omega), \\ &= \mp \frac{\alpha}{(1-\alpha)} F_0, \qquad ((n+\alpha)2T_\Omega \leqslant t < (n+1)2T_\Omega), \end{aligned}$$

with $\alpha = 0.2$ gives an efficiency of 3.8×10^{-2} compared to 6.2×10^{-5} in the symmetric drive ($\alpha = 0$) case with $F_0 = 0.16$ and $2T_\Omega = 1000$. This is made possible because in the symmetric drive case the particles move in either direction with almost equal probability whereas in the asymmetric drive case the particle motion in one direction is practically blocked, as is evident from the corresponding velocity distributions shown in the inset of figure 5. The contribution of the system inhomogeneity for this improved performance is, however, quite insignificant.

3.4. The transient-state dispersions and the ratchet current

When a constant force F is applied to the system it shows dispersionless behaviour: $\langle(\Delta x(t))^2\rangle$ does not change with time in the intermediate timescales, roughly $[10^3 < t < 10^5]$, for around $[0.12 < F < 0.7]$ at $T = 0.4$ for $\gamma_0 = 0.035$. The result of dispersionless behaviour had originally been shown and explained [16] beautifully for the constant friction γ_0 case: the position distribution moves undistorted at constant velocity $v = \frac{F}{\gamma_0}$ or equivalently, the velocity distribution remains undistorted centred at $v = \frac{F}{\gamma_0}$. The interval $[\, t_1 < t < t_2]$ of time during which the system shows this remarkable intermediate-time behaviour depends on the tilt force F, as it should also on other parameters. t_1 is roughly of the order of, but much larger than, the mean Kramers passage time corresponding to the lower of the potential barriers on either side of a well. The transient-time dispersionless particle-motion behaviour is sensitive to initial conditions. In the following we specifically begin from the bottom of the well at $x \approx \frac{\pi}{2}$ with particle velocities given by a Maxwell–Boltzmann distribution at temperature $T = 0.4$.

When the inhomogeneous system is driven periodically by a square-wave forcing of amplitude F_0, the dispersionless coherent nature of average motion gets interrupted, depending on the value of T_Ω of the forcing (figure 6). When $t_1 <$

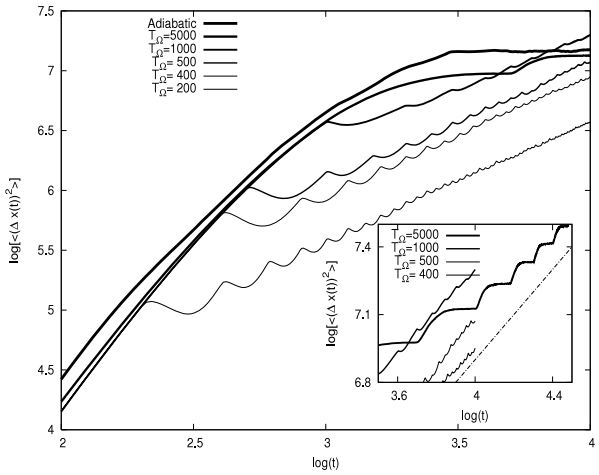

Figure 6. The plot of position dispersions $\langle(\Delta x(t))^2\rangle$ versus time t (in logarithmic scale) for different values of (T_Ω) of forcing with $F_0 = 0.2, \phi = 0.35$. The inset shows the clipped part of the plot at larger time. The dashed line in the inset is drawn just to guide the eye to compare with the diffusive regime.

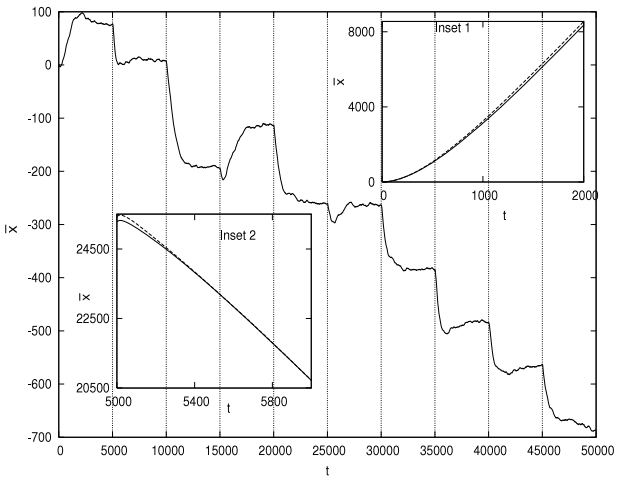

Figure 7. The average displacement of particles as a function of time, driven by equal numbers of $\pm F(t)$ profiles (or equal number of odd and even numbered trajectories) for $T_\Omega = 5000$, $\gamma_0 = 0.035$, $F_0 = 0.2, \phi = 0.35$ and $T = 0.4$. The insets highlight the contributions to the mean displacement of odd (dashed line, beginning with $+|F_0$) and even (solid line) numbered trajectories separately, leading to the main figure. The mean displacements for the even numbered trajectories are shown with a reversed sign.

$T_\Omega < t_2$, at $t = T_\Omega$ the dispersion gets a jerk and shoots up only to get flattened again in another bout of dispersionless regime. This regime also gets a similar jolt after another T_Ω and the process continues for a large number of periods. When the direction of the applied force is changed the 'forward moving' particles are forced individually to halt momentarily to begin moving afresh in the new direction of the force. While in the 'state of halt' particles are more likely to find themselves 'thermalized' to the bottom of some well and thus the system gets initialized as in the beginning. The system finds itself in a similar situation again and again periodically with each change of force direction and continues with its unfinished dispersionless journey for a large number of periods with remarkable robustness (inset of figure 6, $T_\Omega = 5000$). However, when $T_\Omega < t_1$ the system never gets a chance to experience its dispersionless journey because only a fraction of the particles get the opportunity to acquire the required constant average velocity [16] of $\frac{F_0}{\gamma_0}$ and the rest keep lagging behind even by the end of constant force duration T_Ω. Instead, as soon as the direction of the force F is reversed after T_Ω, the dispersion dips after a brief climb up, as the particles get herded together briefly before getting dispersed further in the reversed direction of F_0. This can be seen very clearly in the time evolution of the position probability distribution profile $P(x, t)$. The front of the $P(x, t)$ moves with velocity $\frac{F_0}{\gamma_0}$ while the rest lag behind it moving at a slower speed but trying to catch up with the front throughout T_Ω. This process of dispersion dipping (after a small continuing rise) and rising to a higher value after each T_Ω is repeated for several tens of periods (figure 6).

In the inset of figure 6 we have drawn a straight line with slope 1 as a guide to show that ultimately the curves should achieve that average slope at large times for various T_Ω values of drives. Even though the average slope of the curves have not yet reached the diffusive slope of *one*, the small T_Ω curves are slowly approaching that value. One can, therefore, safely infer that in the steady state situation the effective diffusion constant should increase monotonically with T_Ω for small T_Ω. The frequency of drive, or equivalently T_Ω, thus plays an important role about how the particles diffuse out of their wells. For example, the population of the initial well depletes with time exponentially, $N(t) = N(0)e^{-bt}$, with $b = 0.0023$ for $T_\Omega = 250$ and $b = 0.002$ for $T_\Omega = 500$, for $\gamma_0 = 0.035$ at $T = 0.4$ that we have studied. By the time the well gets effectively exhausted the first particles would have moved further than a thousand potential wells. Of course, this first well itself (as all others) keeps getting repopulated all the time.

The intermediate-time dispersionless motion is not an exclusive characteristic feature of inhomogeneous systems. It is a characteristic feature of an inertial washboard potential system. However, its study in the inertial inhomogeneous system provides a convincing explanation of the variation of ratchet current as a function of T_Ω (inset of figure 1) and helps in finding a criterion to improve the performance of the ratchet.

In figure 7 the displacement of particles, averaged over 1000 ensembles, as a function of time when driven by an equal number of $\pm F(t)$ profiles, is presented for $T_\Omega = 5000$, $\gamma_0 = 0.035$, $F_0 = 0.2$ and $T = 0.4$. This case corresponds to the repeated dispersionless motion shown in figure 6. Figure 7 clearly shows that during the dispersionless motion the average displacement of particles effectively remains constant. In other words, during the period of dispersionless motion the particles move equally in the left as well as in the right direction, thereby contributing nothing to the ratchet current: while in the dispersionless motion the particles fail to see the frictional inhomogeneity of the system. All the change in the average displacement and hence all the contribution to the ratchet current comes during the dispersive period of motion. This is shown in the inset of figure 7 where for clarity the mean particle positions for $F(t)$ beginning with $F(0) = -F_0$ (even

numbered trajectories) are shown as a function of time with their sign reversed. The mean particle displacements for odd and even numbered trajectories differ only during the interval just after the reversal of F_0 and before the dispersionless regime begins and the two lines of mean positions (insets of figure 7) run parallel during the dispersionless regime. This clearly indicates that, in order to get a larger current, an optimum choice of T_Ω needs to be made which, naturally, avoids the dispersionless regime but is not too small in order to allow the particles to leave their potential wells. This conclusion is well supported by the inset of figure 1, where the ratchet current maximizes around $T_\Omega = 500$ which is well below the T_Ω showing dispersionless motion.

The velocity dispersions and position dispersions together show interesting behaviour. Figure 8 shows that during the dispersionless regime when the position dispersion is constant and maximum the velocity dispersion is also constant but it has a minimum value. This minimum constant value is repeated in all the $nT_\Omega, n = 1, 2, \ldots$ intervals whereas the value of the constant position dispersion increases in every successive nT_Ω interval as shown in figure 6 and the inset of figure 8. In the dispersive regimes the velocity dispersions are squeezed to very sharp troughs exactly where the position dispersions show sharp peaking. In the inset of figure 8 these dispersions are shown for $T_\Omega = 250$. The onward rush of the particles do not halt immediately after the direction of F_0 is changed at nT_Ω but it continues for a very short time giving a small increase in the spread of $P(x)$. Then a majority of particles stop, giving a sharp peak in $P(v)$ at $v = 0$, reducing its spread drastically. At that moment the product of position and velocity distribution spread becomes a minimum. The reverse journey thereafter increases the spread of $P(v)$ but there is a slow squeezing of $P(x)$ before it begins to spread again. The maximum $P(x)$ squeezing, however, does not exactly coincide with the largest of the broad $P(v)$ but it is at a rather close range. In this case too the minimum velocity dispersion remains constant for all nT_Ω. But the wings of $P(x)$, though thin, keep spreading with time giving an average increase of dispersion as time increases. However, most of the particles remain confined roughly to a region $[-\frac{|F_0|}{\gamma_0}T_\Omega < x < +\frac{|F_0|}{\gamma_0}T_\Omega]$ for a long time.

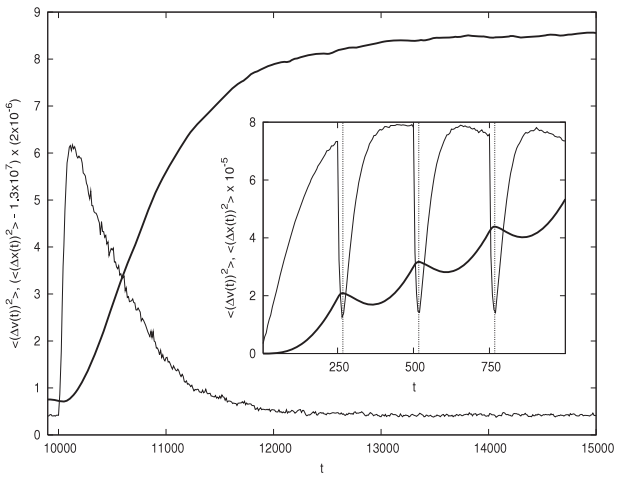

Figure 8. Illustration of velocity dispersions $\langle(\Delta v(t))^2\rangle$ (thin line) and position dispersions $\langle(\Delta x(t))^2\rangle$ (bold line) during a time interval for $T_\Omega = 5000$ and $\phi = 0.35$. The inset shows the corresponding plots for square drive forcing with smaller $T_\Omega = 250$ with no dispersionless regime.

4. Discussion and conclusion

The ratchet effect, in this work, is brought about just by the phase lag ϕ between the periodic potential and the nonuniform friction of the medium, without having to have an overall external bias. This is seemingly a weak cause to generate unidirectional current. Figures 1–5 refer to a square-wave forcing with $T_\Omega = 1000$. The choice of this T_Ω clearly avoids the dispersionless regime. Yet, this is not the optimum value of T_Ω. It should have been around 500 in order to get the largest possible ratchet current. This choice would have definitely enhanced the Stokes efficiency of operation. The same can also be said about other parameters, such as T, and ϕ for $\gamma_0 = 0.035$. Moreover, an optimal choice of all these parameters may possibly help in obtaining a larger ratchet current to obtain useful practical work against an applied load. However, with the help of these figures we have been able to exhibit the qualitative trends shown by the ratchet.

The dispersive behaviour for drives with $T_\Omega > t_2$ is difficult to study because it takes very long computer times to arrive at a concrete result. However, the indications are there that for these large T_Ω also, the system shows repeated dispersionless regimes, though somewhat enfeebled because the process of diffusion will dominate at these large times.

To conclude, the present detailed study reinforces an earlier suggested interesting method [12] of obtaining a ratchet current in inertial noisy systems by exploiting the frictional inhomogeneity of the medium. Moreover, it shows that as the system is driven by a square-wave external forcing of appropriate frequency, dispersionless particle motion could be observed after each field direction change. These transient dispersionless regimes, however, disappear as the frequency is increased and instead periodic variation of dispersions results. The 'moderately high frequency' dispersive regimes (where dispersions vary periodically) help in increasing the ratchet current considerably. Similarly, in these dispersive regimes, the velocity dispersion also varies periodically, with twice the frequency of the field drive, but in exact anti-phase to the position dispersions. In the nondispersive regimes, on the other hand, when the particles move coherently, they tend not to notice the frictional inhomogeneity and do not contribute to the ratchet current. In the present work, however, the ratchet current is obtained when the amplitude of periodic rocking was small. It would be interesting to examine if one could obtain a ratchet current with the help of high amplitude drive as in the case of asymmetric periodic potentials.

Acknowledgments

MCM acknowledges BRNS, Department of Atomic Energy, Government of India, for partial financial support and thanks A M Jayannavar for discussion, and the Abdus Salam ICTP,

Trieste, Italy for providing an opportunity to visit, under the associateship scheme, where a part of this work was completed and the paper was written. We thank CDAC, Pune for allowing us to use their computational facility.

References

[1] Risken H 1996 *The Fokker–Planck Equation* (Berlin: Springer)
Risken H and Vollmer H D 1979 *Z. Phys.* B **33** 277
[2] Machura L, Kostur M, Marchesoni F, Talkner P, Hänggi P and Łuczka J 2005 *J. Phys.: Condens. Matter* **17** S3741
Machura L, Kostur M, Talkner P, Łuczka J, Marchesoni F and Hänggi P 2004 *Phys. Rev.* E **70** 061105
[3] Reimann P 2002 *Phys. Rep.* **361** 57
Feynman R P, Leighton R B and Sands M 1963 *The Feynman Lectures in Physics* vol 1 (Philippines: Addison-Wesley) chapter 46
[4] Machura L, Kostur M, Talkner P, Łuczka J and Hänggi P 2007 *Phys. Rev. Lett.* **98** 040601
Kostur M, Machura L, Talkner P, Hänggi P and Łuczka J 2008 *Phys. Rev.* B **77** 104509
[5] Nagel J, Speer D, Gaber T, Sterck A, Eichhorn R, Reimann P, Ilin K, Siegel M, Koelle D and Kleiner R 2008 *Phys. Rev. Lett.* **100** 217001
[6] Wahnström G 1985 *Surf. Sci.* **159** 311
[7] Falco C M 1976 *Am. J. Phys.* **44** 733
Barone A and Paterno G 1982 *Physics and Applications of the Josephson Effect* (New York: Wiley)
[8] Landauer R 1988 *J. Stat. Phys.* **53** 233
[9] Büttiker M 1987 *Z. Phys.* **68** 161
[10] Blanter Ya M and Büttiker M 1988 *Phys. Rev. Lett.* **81** 4040
[11] Benjamim R and Kawai R 2008 *Phys. Rev.* E **77** 051132
[12] Reenbohn W L, Saikia S, Roy R and Mahato M C 2008 *Pramana J. Phys.* **71** 297
[13] Reenbohn W L and Mahato M C 2009 *J. Stat. Mech.* P03011 (arXiv:0807.2725)
[14] Lindner B, Kostur M and Schimansky-Geier L 2001 *Fluct. Noise Lett.* **1** R25
[15] Sekimoto K 1997 *J. Phys. Soc. Japan* **66** 6335
[16] Lindenberg K, Sancho J M, Lacasta A M and Sokolov I M 2007 *Phys. Rev. Lett.* **98** 020602
[17] Press W H, Teukolsky S A, Vetterling W T and Flannery B P 1992 *Numerical Recipes (in Fortran): the Art of Scientific Computing* (Cambridge: Cambridge University Press)
Mahato M C and Shenoy S R 1993 *J. Stat. Phys.* **73** 123
[18] Borromeo B, Constantini G and Marchesoni F 1999 *Phys. Rev. Lett.* **82** 2820
Mahato M C and Jayannavar A M 2003 *Physica* A **318** 154